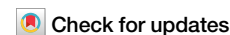





<https://doi.org/10.1038/s42003-024-07438-1>

Function of orexin-1 receptor signaling in the olfactory tubercle in odor-guided attraction and aversion



Md Monjurul Ahasan, Md Tasnim Alam, Yoshihiro Murata , Mutsuo Taniguchi & Masahiro Yamaguchi  

While olfactory behaviors are influenced by neuromodulatory signals, the underlying mechanism remains unknown. The olfactory tubercle (OT), a component of the olfactory cortex and ventral striatum, consists of anteromedial (am) and lateral (l) domains regulating odor-guided attractive and aversive behaviors, respectively, in which the amOT highly expresses various receptors for feeding-regulated neuromodulators. Here we show functions of appetite-stimulating orexin-1 receptor (OxR1) signaling in the amOT. When odor-food reward associated mice underwent OxR1 antagonist injection in the amOT, their odor-attractive behavior was suppressed and odor-aversive behavior was conversely induced. Although odor-attractive mice showed activation of attraction-promoting dopamine receptor type 1-expressing D1 cells in the amOT, the antagonist injection increased activation of aversion-promoting D2 cells in the amOT and D1 cells in the lOT. The results highlight the amOT as the crucial structure integrating OxR1 signaling and odor information, thereby controlling metabolic status-dependent olfactory behavior through the cell type- and domain-specific activation.

Odor information induces a variety of behaviors important for sustaining the life of animals, one of which is feeding behavior^{1,2}. Feeding behavior involves a variety of functional systems—including the nervous system, digestive system, and endocrine system—and is regulated by their interactions^{3,4}. Olfactory function such as odor sensitivity is strongly influenced by metabolic status^{5,6}. Regarding odor-guided feeding behavior, although food odor elicits appetite when we are hungry, the same odor does not induce appetite and sometimes elicits nausea when we are satiated. However, the neural mechanisms underlying the influence of metabolic status on odor valence and olfactory behavior are unknown.

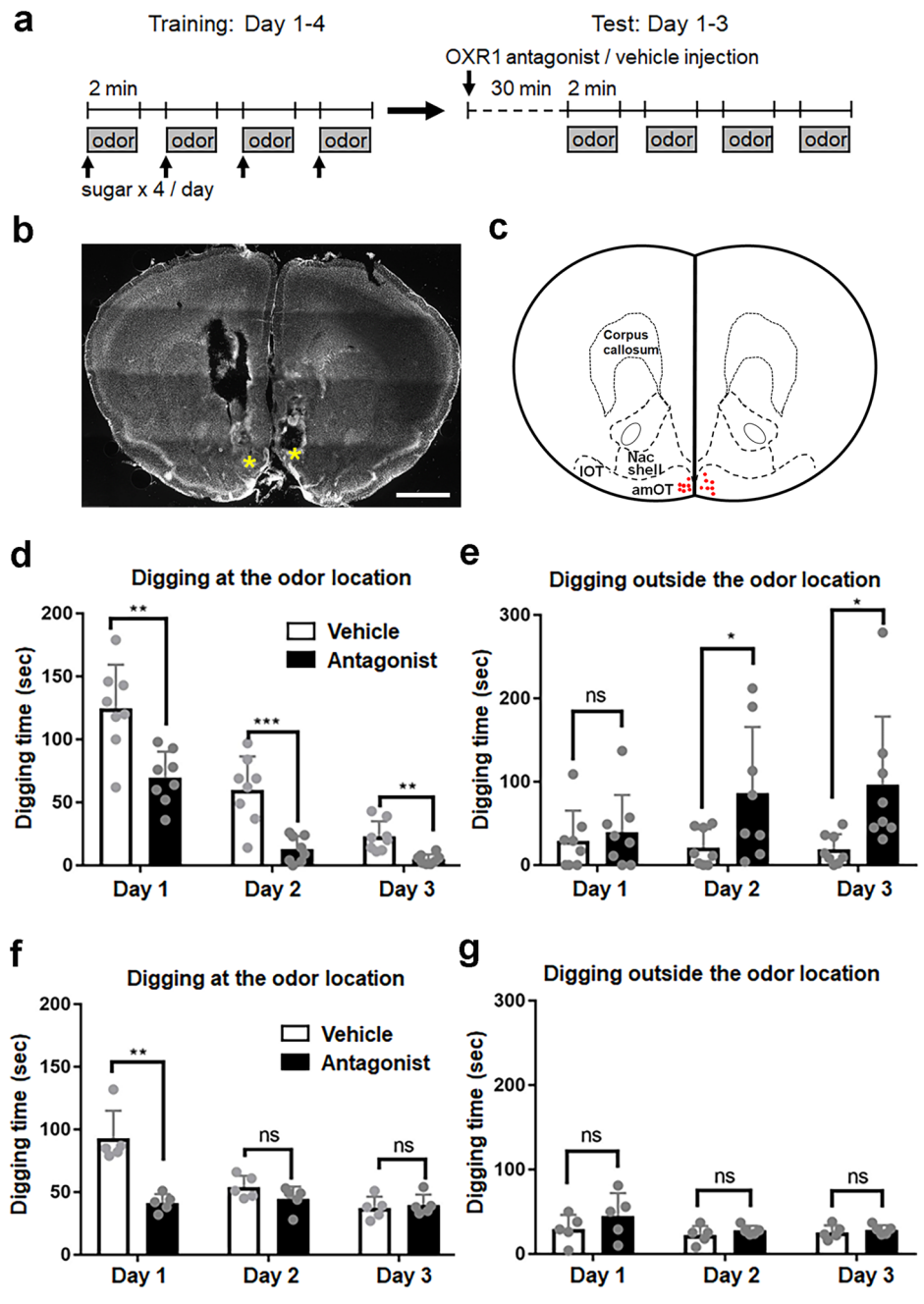
Odor information is received by the olfactory sensory neurons in the olfactory epithelium and transferred via the olfactory bulb to the olfactory cortex. The olfactory cortex comprises several structures including the anterior olfactory nucleus, olfactory tubercle (OT), piriform cortex, cortical amygdala, and entorhinal cortex⁷. Among them, the OT, which is also called the tubular striatum, is a unique area in that it constitutes the ventral striatum with the nucleus accumbens (NAc) and receives massive dopaminergic inputs from the midbrain^{8–10}. In agreement with these structural properties, the OT encodes odor valence and contributes to numerous odor-guided behaviors^{11–14}. The important function of the OT in olfactory behaviors raises the possibility that it receives information on metabolic status and optimizes odor-guided feeding behaviors accordingly.

The OT has domain structures associated with odor-guided motivated behaviors. In mice that have associated a neutral odor with a food reward and have become attracted to the learned odor, presentation of the odor activates the anteromedial domain of the OT (amOT). By contrast, in mice that have associated the same odor with a foot-shock punishment and have become aversive to the odor, presentation of the odor activates the lateral domain of the OT (lOT)¹⁴. Intriguingly, a variety of receptors for feeding-related neuromodulators are expressed at higher levels in the OT, especially in the amOT and the central part of the OT, compared to the lOT¹⁵. These observations suggest the amOT to be a key brain region that coordinates odor information and metabolic status and directs appropriate feeding behavior.

Orexin, a feeding-related neuromodulator, is an orexigenic neuropeptide that promotes motivational and reward-seeking behaviors^{16–18}. Orexin is produced in the lateral hypothalamus by orexin neurons, which project axons to other brain areas¹⁹. There are two types of orexin receptors—orexin-1 receptor (OxR1) and orexin-2 receptor (OxR2)²⁰. These receptors are reported to be expressed in the rodent OT^{21–23}, and we showed using quantitative RT-PCR that expression of *OxR1* and *OxR2* mRNA are higher in the amOT than the lOT, with a greater extent of the domain difference for *OxR1* than *OxR2*¹⁵. Given this highly preferential expression of *OxR1* in the amOT and the notion that reward-related behaviors are more closely associated with the activation of OxR1 than OxR2¹⁷, here we focused on the

Department of Physiology, Kochi Medical School, Kochi University, Kochi, Japan. ✉ e-mail: yamaguchi@kochi-u.ac.jp

Fig. 1 | Suppression of odor-attractive behavior by local injection of an OxR1 antagonist into the amOT. **a** Protocol for odor-sugar association training and behavioral analysis following OxR1 antagonist injection. Food-restricted mice received association training with an odor (eugenol) and sugar for 4 days (training: days 1–4). The mice underwent injection of an OxR1 antagonist (SB334867) or vehicle in the bilateral amOT and were examined for odor-guided behavior for 3 days (test: days 1–3). **b, c** Placement of drug cannulae in the amOT. **b** Coronal section of the OT. Asterisk, position of the cannula tip. Scale bar, 1 mm. **c** Schematic of cannula placement (red dots; $n = 7$ representative mice). **d, e** Odor-guided behavior of mice during test days 1–3. **d** Digging behavior at the odor location. **e** Digging behavior outside the odor location. Digging time within four 2 min-trials of vehicle-injected mice (white columns) and antagonist-injected mice (black columns). **f, g** Odor-guided behavior during test on days 1–3, in mice that received vehicle/antagonist injection only on day 1. **f** Digging behavior at the odor location. **g** Digging behavior outside the odor location. Digging time within four 2 min-trials of vehicle-injected mice (white columns) and antagonist-injected mice (black columns). In **d–g** average \pm SD are shown. Each dot represents one mouse ($n = 8$ mice for both groups in **d, e; $n = 5$ mice for both groups in **f, g**). ns not significant; * $p < 0.05$; ** $p < 0.01$; *** $p < 0.001$ (unpaired t -test).**



role of OxR1 signaling in the amOT. We conducted local injection of an OxR1 antagonist into the OT domains of mice and evaluated the effect on their odor-guided appetitive behavior.

The principal neurons in the OT are medium spiny neurons, which consist of dopamine receptor type 1-expressing (D1) cells and type 2-expressing (D2) cells; these cell types have distinct functional properties in odor-guided behaviors^{14,24–26}. Odor-attractive behavior is accompanied by activation of D1 cells in the amOT and odor-aversive behavior is accompanied by activation of D1 cells in the IOT¹⁴. Conversely, activation of D2 cells in the amOT induces aversive behavior²⁷. Given that odor-guided behaviors are regulated by domain-specific and cell type-specific activation in the OT, we investigated the effect of an OxR1 antagonist on domain- and cell type-specific activation in the OT. Our results show that blockade of OxR1 signaling in the amOT by local antagonist injection converts odor valence from attraction to aversion and that this conversion accompanies activation of D2 cells in the amOT and D1 cells in the IOT.

Results

Local injection of OxR1 antagonist into the amOT suppressed odor-attractive behavior and induced aberrant behavior to the cue odor

Figure 1a shows the schedule of the behavioral analysis. Mice under food restriction received association training on a cue odor (eugenol) and sugar reward for 4 days. They were subsequently injected with SB334867, an OxR1-specific antagonist, or vehicle via cannulae implanted in the bilateral amOT (Supplementary Fig. 1 for local injection procedure). Correct positioning of the cannulae was confirmed histologically after completion of the behavioral analyses (Fig. 1b, c); the data of mice with inappropriate cannula positioning were omitted from the analysis.

On day 1 of the test period, 30 min after antagonist/vehicle injection, mice were transferred to test cages in which a eugenol-scented dish (without sugar) was buried under the bedding on one side. Vehicle-injected mice extensively investigated the location where the cue-odor was buried (digging

at the odor location) (Fig. 1d, Supplementary Movie 1). By contrast, the antagonist-injected mice spent less time investigating the odor location ($F_{(1, 14)} = 31.3$, $p < 0.001$ for injection, $F_{(2, 28)} = 4.49$, $p = 0.020$ for interaction, two-way ANOVA; $p = 0.0017$, t -test for day 1). The same procedure was conducted on the next 2 days (test days 2 and 3). During the 3 days of the test period, the digging time at the odor location gradually decreased for vehicle- and antagonist-injected mice ($F_{(2, 28)} = 87.6$, $p < 0.001$ for day, two-way ANOVA), which was considered an extinction or re-learning of the odor-sugar association because only the cue odor without sugar was presented during the test period. Even accounting for the decrease in odor-investigation behavior, the antagonist injection suppressed odor-attractive behavior for 3 days (test day 2, $p = 0.0003$; test day 3, $p = 0.0012$; t -test). Further, the percentage of digging time at the odor location of antagonist-injected mice versus vehicle-injected mice was calculated by comparing average digging time. The values were 55.8% (69.6 s / 124.8 s) on day 1, 21.4% (12.9 s / 60.2 s) on day 2, and 21.2% (4.9 s / 23.1 s) on day 3, indicating the potentiation of the suppressive effect of antagonist injection along 3 days.

Intriguingly, antagonist-injected mice showed an aberrant behavior; they dug the bedding extensively outside the location of the cue odor (digging outside the odor location). Typically, they dug the bedding on the side opposite the odor location ($F_{(1, 14)} = 4.73$, $p = 0.047$ for injection, $F_{(2, 28)} = 5.08$, $p = 0.013$ for interaction, two-way ANOVA; Fig. 1e; Supplementary Movie 2). Such behavior significantly increased on test days 2 and 3 (test day 1, $p = 0.61$; test day 2, $p = 0.043$; test day 3, $p = 0.021$; t -test). This aberrant behavior was potentiated during the 3 days; the percentage of average digging time outside the odor location of antagonist-injected mice versus vehicle-injected mice was 136.7% (39.5 s / 28.9 s) on day 1, 409.0% (86.3 s / 21.1 s) on day 2, and 507.4% (96.4 s / 19.0 s) on day 3.

As a basis for the potentiation of digging behaviors during repeated OxR1 antagonist injection, we examined whether the effect of a single OxR1 injection was maintained over days. The mice were injected with an OxR1 antagonist only on day 1, and behavioral tests were conducted on days 1–3. On day 1, the digging time at the odor location was suppressed in antagonist-injected mice compared to vehicle-injected mice ($F_{(1, 8)} = 21.56$, $p = 0.002$ for injection, $F_{(2, 16)} = 13.48$, $p < 0.001$ for interaction, two-way ANOVA; test day 1, $p = 0.0011$, t -test; Fig. 1f). However, this suppressive effect was lost on days 2 and 3 (test day 2, $p = 0.16$; test day 3, $p = 0.67$; t -test). The digging time outside the odor location was not enhanced in the antagonist-injected mice on day 1, nor on day 2 or 3, contrary to the Fig. 1e case ($F_{(1, 8)} = 1.53$, $p = 0.25$ for injection, $F_{(2, 16)} = 0.74$, $p = 0.49$ for interaction, two-way ANOVA; test day 1, $p = 0.30$; test day 2, $p = 0.36$; test day 3, $p = 0.52$; t -test; Fig. 1g).

Taken together, local injection of the OxR1 antagonist in the amOT suppressed digging behavior at the cue odor location and conversely induced digging behavior outside the cue odor location, and these effects were not sustained over a day but were gradually potentiated by repeated injections across days. Digging behavior is promoted by a variety of factors^{28,29}. Digging at the odor location is considered to be a food-searching behavior^{14,30}. The digging behavior of antagonist-injected mice outside the odor location could be search for food in places away from the cue odor, or protection against the cue odor because it resembled burrowing behavior to shelter from danger^{29,31,32}. These observations indicated that local injection of an orexin receptor type 1-antagonist in the amOT suppressed odor-attractive behavior and suggested that the manipulation conversely induced aversive behavior in response to the cue odor.

Local injection of an OxR1 antagonist into the amOT converted the odor valence from attraction to aversion

To evaluate whether antagonist-injected mice were aversive to the cue odor, their behavior was evaluated after removing the paper bedding from the cage to prevent complex digging behavior. On test day 4, mice were habituated to the bedding-free cage, injected with antagonist or vehicle into the amOT, and presented with the cue odor.

Vehicle-injected mice showed extensive investigative behavior towards the odor (Fig. 2a, Supplementary Movie 3). By contrast, antagonist-injected mice spent less time investigating the odor, as did vehicle-injected control mice that did not receive odor-sugar association training ($F_{(2, 13)} = 20.42$, $p < 0.0001$, one-way ANOVA; Supplementary Table 1 for multiple comparisons). Further, the antagonist-injected mice showed retraction from the cue odor (Fig. 2b, Supplementary Movie 4). They first approached the odor with their body in longitudinal extension, and rapidly retracted the head and body from the odor (whole-body flinch). Such behavior was rarely observed in the vehicle-injected mice or vehicle-injected control mice that did not receive odor-sugar association training ($F_{(2, 13)} = 125.5$, $p < 0.0001$; Supplementary Table 1). In accordance with these behaviors, vehicle-injected mice spent longer on the odor side of the cage (zone 1) during the test period, and antagonist-injected mice spent longer on the opposite side (zone 2) compared to vehicle-injected mice ($p = 0.0021$, t -test; Fig. 2c). These data indicate that injection of antagonist in the amOT had induced aversion to the cue odor.

To examine whether the shift of the odor valence from attraction to aversion caused by the antagonist is dependent on metabolic status, the mice were supplied with sufficient food following the day-4 test. After ~24 h of *ad libitum* feeding, the body weight of the mice was similar to before food restriction. The body weights of antagonist-injected mice just before food restriction, during food restriction (test day 4), and after 1 day of *ad libitum* feeding (test day 5) were 25.8 ± 1.3 g, 22.1 ± 1.3 g (85.5 ± 2.6% of that just before food restriction), and 25.2 ± 1.8 g (97.5 ± 3.2% of that just before food restriction; $n = 6$), respectively, and those of vehicle-injected mice were 26.5 ± 1.3 g, 22.4 ± 0.9 g (84.6 ± 4.1% of that just before food restriction), and 25.1 ± 1.3 g (94.7 ± 5.1% of that just before food restriction; $n = 5$), respectively. On test day 5, the behavior of the mice was examined under the bedding-free condition. Similar to test day 4, antagonist-injected mice showed reduced investigation to the cue odor ($F_{(2, 13)} = 46.61$, $p < 0.0001$; Fig. 2d; Supplementary Table 1) and increased retraction from the cue odor ($F_{(2, 13)} = 12.64$, $p = 0.0009$; Fig. 2e; Supplementary Table 1) and spent less time in the odor-side zone compared to vehicle-injected mice ($p = 0.040$; Fig. 2f).

To further confirm the effect of metabolic status on the change in odor-cued digging behaviors after OxR1 antagonist injection, mice were trained to associate the cue odor with a sugar reward for 4 days under food restriction and then were supplied with sufficient food. The digging behavior of the mice in response to presentation of the odor under the *ad libitum* feeding condition was examined (test days 1–3; Fig. 2g, h). While the digging time at the odor location was relatively short compared to that under food restriction (see Fig. 1d), the antagonist significantly suppressed digging behavior ($F_{(1, 8)} = 176.17$, $p < 0.001$ for injection, $F_{(2, 16)} = 10.36$, $p = 0.0010$ for interaction, two-way ANOVA; test day 1, $p < 0.001$; test day 2, $p = 0.019$; test day 3, $p = 0.012$; t -test; Fig. 2g). Intriguingly, digging outside the odor location was not enhanced by antagonist injection ($F_{(1, 8)} = 0.91$, $p = 0.37$ for injection, $F_{(2, 16)} = 0.076$, $p = 0.93$ for interaction, two-way ANOVA; test day 1, $p = 0.75$; test day 2, $p = 0.27$; test day 3, $p = 0.53$; t -test; Fig. 2h). This indicates that the aberrant digging behavior away from the cue odor depended on metabolic status and became evident only under food restriction (see Discussion). The mice were presented with the cue odor in the bedding-free cage on test day 4. The odor-investigating behavior in vehicle-injected mice was suppressed in the antagonist-injected mice ($p = 0.028$, t -test; Fig. 2i), and the odor-retracting behavior was significantly potentiated in those mice ($p < 0.001$, t -test; Fig. 2j). In this case, the ratio of residence either on the odor side of the cage (zone 1) or on the opposite side (zone 2) was not significantly different ($p = 0.39$, t -test; Fig. 2k); the reason remains unclear but it may be due to attenuated odor-investigating motivation under the prolonged well-fed condition. The body weights of antagonist-injected mice just before food restriction, during food restriction (training day 4), after 1 day of *ad libitum* feeding (test day 1) and after 4 day of *ad libitum* feeding (test day 4) were 24.4 ± 0.5 g, 19.9 ± 0.7 g (81.6 ± 2.7% of that just before food restriction), 22.9 ± 0.8 g (93.6 ± 2.1% of that just before food restriction), and 22.3 ± 0.9 g (91.7 ± 5.3% of that just before food

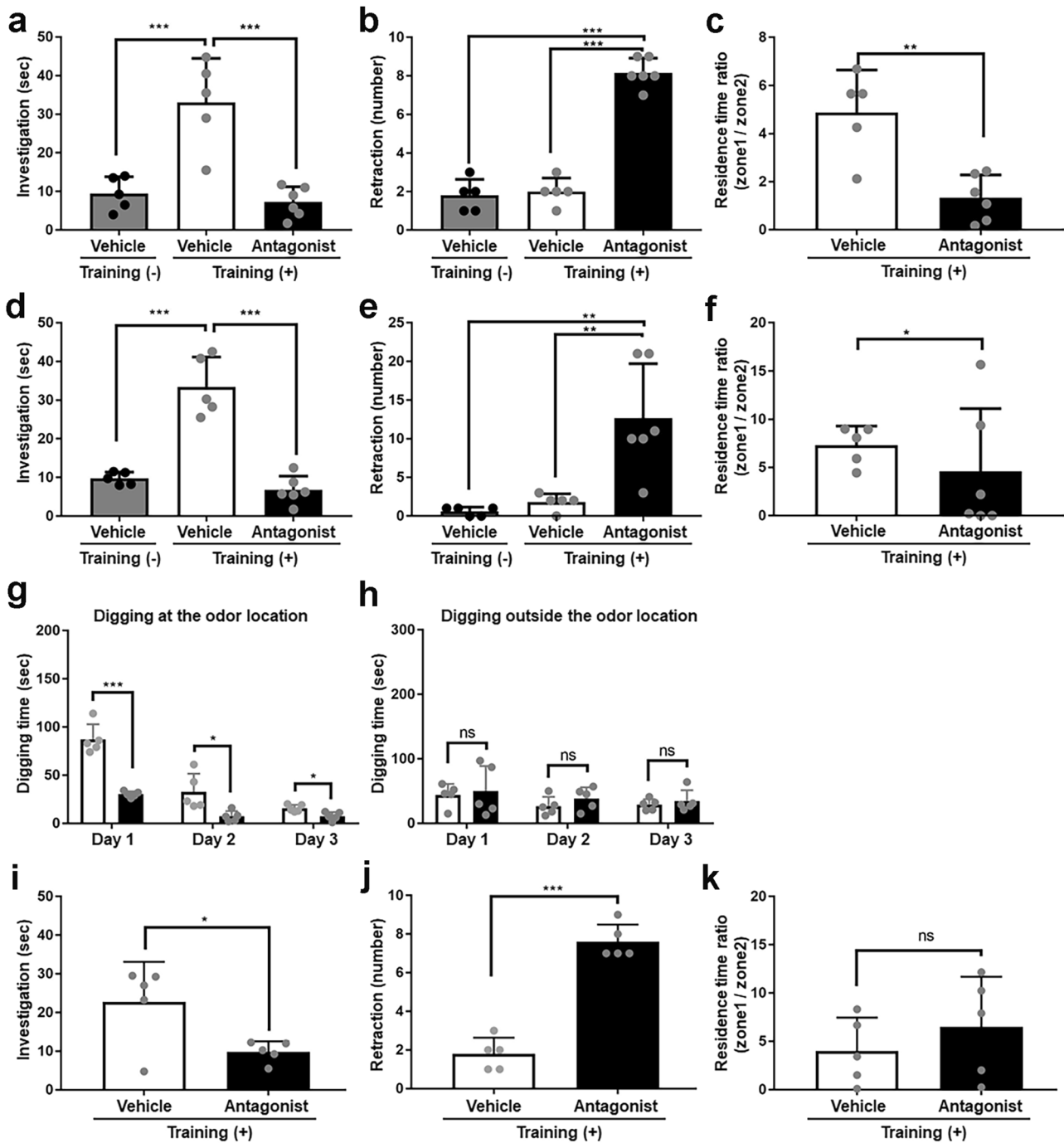


Fig. 2 | Conversion of odor valence by local injection of an OxR1 antagonist into the amOT. **a–c** Odor-guided behavior of food-restricted mice under the bedding-free condition. **a** Odor-investigating time within 2 min of vehicle-injected mice (white column), antagonist-injected mice (black column), and vehicle-injected control mice that did not receive odor-sugar association training (gray column). **b** Occurrence of odor-retraction within 2 min of three groups of mice. **c** Ratio of residence times on the odor side (zone 1) versus the opposite side (zone 2) of vehicle-injected and antagonist-injected mice. **d–f** Odor-guided behavior of *ad libitum*-fed mice under the bedding-free condition. **d** Odor-investigating time within 2 min of vehicle-injected, antagonist-injected, and vehicle-injected control mice that did not receive odor-sugar association training. **e** Occurrence of odor-retraction within 2 min of three groups of mice. **f** Ratio of residence times on the odor side (zone 1) versus the opposite side (zone 2) of vehicle-injected and antagonist-injected mice.

g–k Odor-guided behavior of mice well-fed following 4 days of odor-sugar association training. **g, h** Odor-guided behavior of mice during test days 1–3. **g** Digging behavior at the odor location. **h** Digging behavior outside the odor location. Digging time within four 2 min-trials of vehicle-injected mice (white columns) and antagonist-injected mice (black columns). **i** Odor-investigating time within 2 min of vehicle-injected and antagonist-injected mice. **j** Occurrence of odor-retraction within 2 min of two groups of mice. **k** Ratio of residence times on the odor side (zone 1) versus the opposite side (zone 2) of two groups of mice. Average \pm SD, each dot represents one mouse ($n = 5$ for control mice, 5 for vehicle-injected mice, 6 for antagonist-injected mice in **a–f**; $n = 5$ for both groups of mice in **g–k**). ns not significant; * $p < 0.05$; ** $p < 0.01$; *** $p < 0.001$ (one-way ANOVA with Tukey’s multiple comparisons test for **a, b, d, e**; *t*-test for **c, f, g–k**).

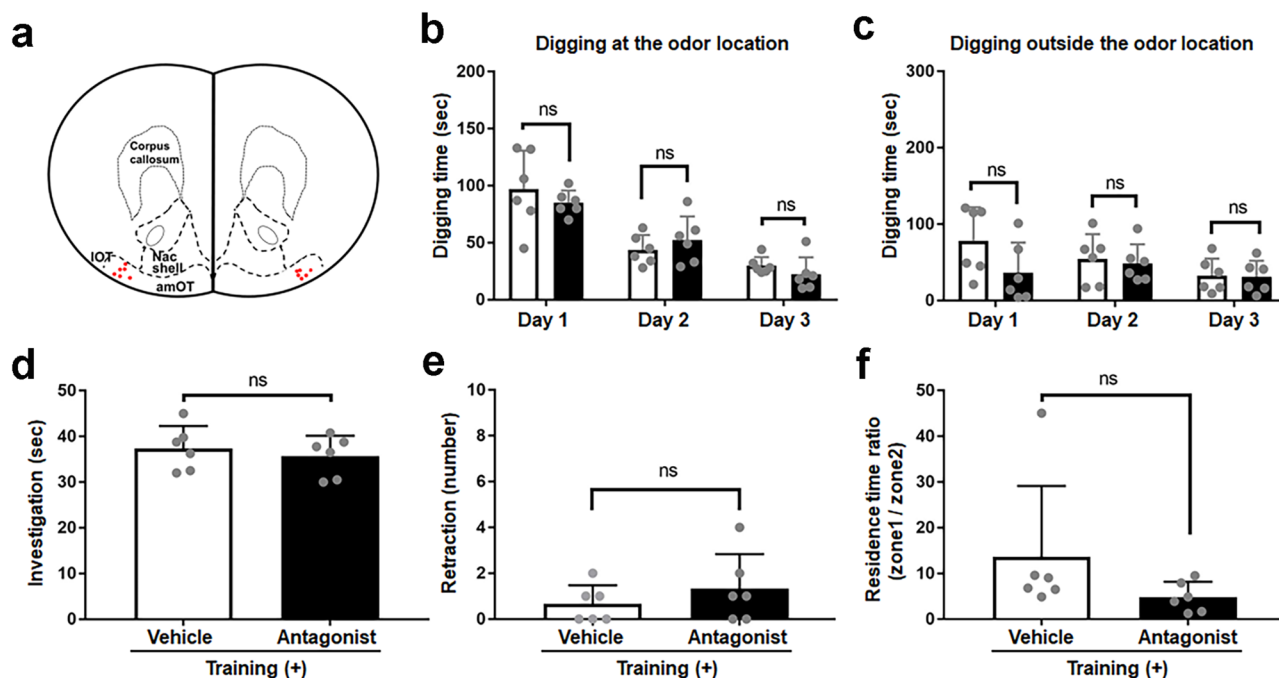


Fig. 3 | Odor-attractive behavior is not significantly influenced by the local injection of an OxR1 antagonist into the IOT. **a** Schematic of cannula placement (red dots; $n = 6$ representative mice). **b, c** Odor-guided behavior of mice during test days 1–3. **b** Digging behavior at the odor location. **c** Digging behavior outside the odor location. **d** Odor-investigating behavior of *ad libitum*-fed mice under the

bedding-free condition. **e** Odor-retraction behavior of *ad libitum*-fed mice under the bedding-free condition. **f** Ratio of residence time on the odor side (zone 1) versus the opposite side (zone 2). White columns, vehicle-injected mice; black columns, antagonist-injected mice. Average \pm SD, each dot represents one mouse ($n = 6$ mice for both groups). ns, not significant (*t*-test).

restriction), respectively, and those of vehicle-injected mice were 23.4 ± 0.4 g, 19.7 ± 0.5 g ($84.5 \pm 3.2\%$ of that just before food restriction), 23.4 ± 0.6 g ($100.4 \pm 4.1\%$ of that just before food restriction), and 22.8 ± 0.6 g ($97.8 \pm 2.1\%$ of that just before food restriction), respectively.

While the meanings of aberrant digging behavior and residence preference remain elusive, the consistent appearance of odor-retraction behavior even under the prolonged well-fed condition indicates that the OxR1 antagonist injection into the amOT shifted the odor valence from attraction to aversion, an effect not significantly altered by metabolic status.

Local injection of an OxR1 antagonist into the IOT or NAc shell did not affect odor-guided attractive behavior

To examine whether the effect of the antagonist on odor-guided behavior was dependent on its injection into the amOT, mice were implanted with drug cannulae in the bilateral IOT or NAc shell and subjected to behavioral analysis. The correct positioning of cannulae was confirmed histologically after completion of the behavioral analysis (Figs. 3a and 4a).

Injection of the antagonist into the IOT did not significantly influence attractive behavior to the cue odor. On test days 1–3, the mice extensively dug the bedding over the odor location and their digging behavior outside the odor location was similar to vehicle-injected mice (digging at the odor location, $F_{(1, 10)} = 0.29$, $p = 0.60$ for injection, $F_{(2, 20)} = 1.07$, $p = 0.36$ for interaction, two-way ANOVA; $p = 0.43$, 0.41 and 0.29 for days 1, 2 and 3, respectively, *t*-test; Fig. 3b) (digging outside the odor location, $F_{(1, 10)} = 1.55$, $p = 0.24$ for injection, $F_{(2, 20)} = 1.84$, $p = 0.19$ for interaction, $p = 0.12$, 0.73 and 0.90 for days 1, 2 and 3, respectively; Fig. 3c). The behavior of the mice under the bedding-free condition was examined after ~ 24 h of *ad libitum* feeding. They extensively investigated the odor, as did vehicle-injected mice ($p = 0.59$; Fig. 3d), and did not show significant retraction behavior to the cue odor ($p = 0.36$; Fig. 3e). The rate of residence on the odor side versus the opposite side was not significantly different between antagonist- and vehicle-injected mice ($p = 0.20$; Fig. 3f).

Similarly, injection of the antagonist into the NAc shell did not influence the odor-attractive digging behavior (digging at the odor location,

$F_{(1, 10)} = 0.054$, $p = 0.82$ for injection, $F_{(2, 20)} = 0.21$, $p = 0.81$ for interaction, $p = 0.79$, 0.70 and 0.65 for days 1, 2 and 3, respectively; Fig. 4b) (digging outside the odor location, $F_{(1, 10)} = 1.31$, $p = 0.28$ for injection, $F_{(2, 20)} = 0.008$, $p = 0.99$ for interaction, $p = 0.47$, 0.52 and 0.23 for days 1, 2 and 3, respectively; Fig. 4c), or odor investigation ($p = 0.90$; Fig. 4d), odor retraction ($p = 0.72$; Fig. 4e) or residence side ($p = 0.055$; Fig. 4f) under the bedding-free condition. Therefore, the effect of the OxR1 antagonist on odor-attractive and -aversive behavior was dependent on its injection into the amOT.

Local injection of an OxR1 antagonist into the amOT converted unassociated odor valence from neutral to aversion

To examine whether conversion of odor valence by injecting the OxR1 antagonist in the amOT is specific to the association-learned attractive odor, the effect on a neutral odor without association learning was examined. The same odor (eugenol) was presented to food-restricted mice without a sugar reward for 4 days. Then, the behavior of the mice to the odor presentation was examined following OxR1 antagonist or vehicle injection into the amOT (Fig. 5).

The digging times at the odor location for the vehicle-injected and antagonist-injected mice on days 1–3 were short compared to that for the odor-reward associated mice, and were not significantly different between the groups ($F_{(1, 8)} = 5.01$, $p = 0.056$ for injection, $F_{(2, 16)} = 3.54$, $p = 0.053$ for interaction, two-way ANOVA; test day 1, $p = 0.059$; test day 2, $p = 0.38$; test day 3, $p = 0.12$; *t*-test; Fig. 5a). The digging time outside the odor location was also short in both groups of mice on days 1–3 with no significant difference between the groups ($F_{(1, 8)} = 0.091$, $p = 0.77$ for injection, $F_{(2, 16)} = 1.17$, $p = 0.34$ for interaction, two-way ANOVA; test day 1, $p = 0.96$; test day 2, $p = 0.27$; test day 3, $p = 0.53$; *t*-test; Fig. 5b). However, investigation time was suppressed by antagonist injection on day 5 (well-fed condition; $p = 0.018$, *t*-test; Fig. 5f) but not on day 4 (food-restricted condition; $p = 0.33$, Fig. 5c), and retraction increased significantly in the antagonist-injected mice on day 4 ($p < 0.001$; Fig. 5d) and day 5 ($p < 0.001$; Fig. 5g). The ratio of residence either on the odor side of the cage (zone 1) or on the opposite side (zone 2) was not significantly different on either day

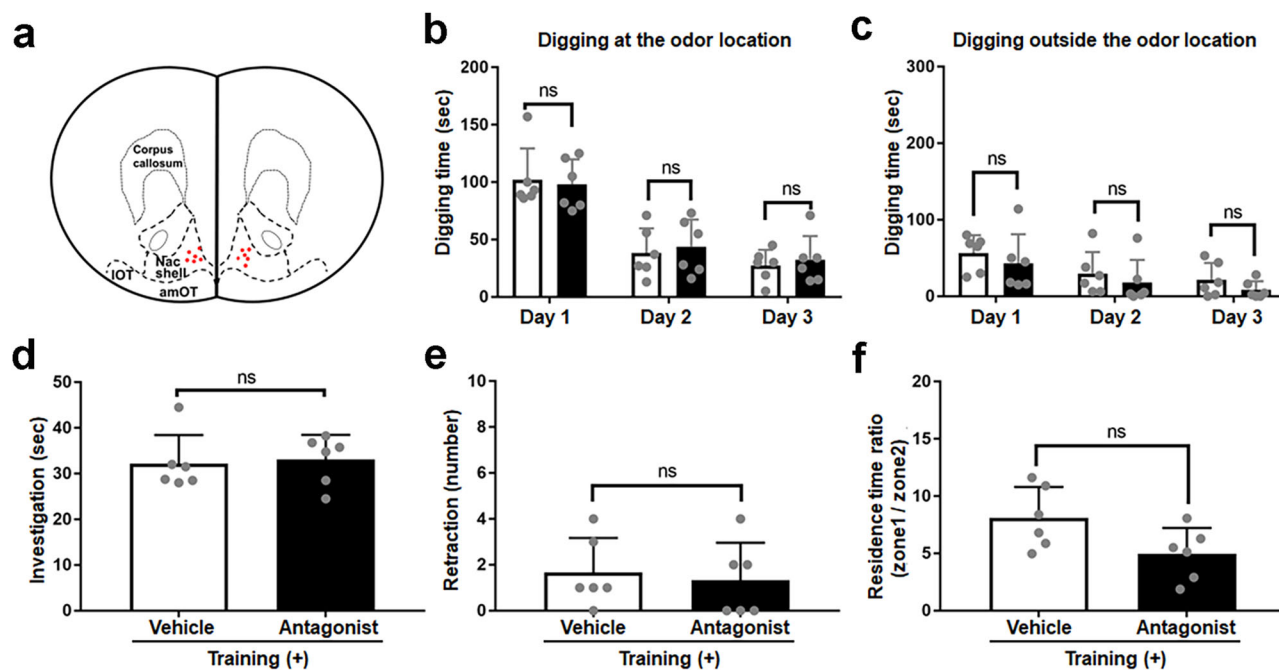


Fig. 4 | Odor-attractive behavior is unaffected by local injection of an OxR1 antagonist into the NAc shell. a Schematic of cannula placement (red dots; $n = 6$ representative mice). **b, c** Odor-guided behavior of mice during test days 1–3. **b** Digging behavior at the odor location. **c** Digging behavior outside the odor location. **d** Odor-investigating behavior of *ad libitum*-fed mice under the bedding-free

condition. **e** Odor-retraction behavior of *ad libitum*-fed mice under the bedding-free condition. **f** Ratio of residence time on the odor side (zone 1) versus the opposite side (zone 2). White columns, vehicle-injected mice; black columns, antagonist-injected mice. Average \pm SD, each dot represents one mouse ($n = 6$ mice for both groups). ns, not significant (*t*-test).

($p = 0.40$, Fig. 5e; $p = 0.25$, Fig. 5h); the reason was unclear but may have been caused by the less odor-investigating motivation toward the unassociated neutral odor. These observations indicate that local OxR1 antagonist injection into the amOT converted the valence of unassociated odor from neutral to aversion.

Injection of an OxR1 antagonist into the amOT affected cell type and domain activation in the OT

Odor-guided attractive and aversive behaviors are accompanied by activation of D1 cells in the amOT and IOT, respectively¹⁴. Further, activation of D1 cells in the amOT is attractive whereas activation of D2 cells in the amOT is aversive²⁷. We here examined how injection of the OxR1 antagonist into the amOT affected cell type- and domain-specific activation in the OT. On the day after completion of the behavioral analysis, mice were injected with OxR1 antagonist or vehicle into the bilateral amOT. After confirming their aversive or attractive behavior to the cue odor, the mice were perfusion-fixed ~ 1 h after the start of odor presentation. Double in situ hybridization (ISH) for *c-Fos* mRNA and *D1/D2* mRNA was performed to evaluate activation of D1/D2 cells in the amOT/IOT in vehicle- and antagonist-injected mice.

Figure 6a, b shows the *c-Fos*(+) cell density in the OT domains of vehicle-injected and antagonist-injected mice. In antagonist-injected mice that showed odor-aversive behavior, the *c-Fos*(+) cell densities were significantly increased both in the amOT and IOT compared to vehicle-injected mice ($F_{(3, 24)} = 8.75$, $p = 0.0004$, one-way ANOVA; Supplementary Table 2 for multiple comparisons), indicating the activation of both amOT and IOT neurons in antagonist-injected mice.

Analysis of double ISH for *c-Fos* mRNA and *D1/D2* mRNA showed that the *c-Fos/D1*(+) cell density in the amOT was not significantly different between vehicle-injected mice and antagonist-injected mice (Fig. 6c, d; $F_{(7, 48)} = 9.79$, $p < 0.0001$, one-way ANOVA; Supplementary Table 2 for multiple comparisons). By contrast, *c-Fos/D2*(+) cell density in the amOT was significantly increased in antagonist-injected mice compared to vehicle-injected mice. Analysis of ratios of *c-Fos/D1*(+) cell density versus *c-Fos/D2*(+) cell density in the amOT within individual mice showed that the ratios for vehicle-injected mice were larger than 1, while those for

antagonist-injected mice were smaller than 1, indicating that the D1(+) cell-dominant activation in vehicle-injected mice converted to D2(+) cell-dominant activation in antagonist-injected mice ($p = 0.004$; Fig. 6e).

In the IOT, the *c-Fos/D1*(+) cell density of antagonist-injected mice was significantly increased compared to vehicle-injected mice (Fig. 6d; Supplementary Table 2). By contrast, *c-Fos/D2*(+) cell density was not significantly different between vehicle-injected and antagonist-injected mice. Analysis of ratios of *c-Fos/D1*(+) cell density versus *c-Fos/D2*(+) cell density in the IOT within individual mice showed that the ratios for vehicle-injected and antagonist-injected mice were larger than 1, and that the values were higher in antagonist-injected mice compared to vehicle-injected mice ($p = 0.0065$; Fig. 6f), indicating that D1(+) cells were preferentially activated in the IOT of antagonist-injected mice.

The above findings indicate that injection of an OxR1 antagonist into the amOT induced D2 cell-dominant activation in the amOT and D1 cell-dominant activation in the IOT. Therefore, injection of the antagonist in the amOT affected cell type- and domain-specific activation in the OT, consistent with the functions of D1/D2 cells in the am/IOT domains^{14,27}.

Discussion

We showed that local injection of an OxR1 antagonist into the amOT, but not the IOT or NAc shell, converted the odor valence from attraction to aversion. This was not significantly influenced by the metabolic status of the mice, such as when hungry or satiated. The conversion of odor valence also occurred for an odor without learning by association. Injection of the antagonist activated D2 cells in the amOT and D1 cells in the IOT, consistent with the behavioral changes. Our findings suggest that the amOT coordinates odor information and metabolic signals to optimize feeding behavior.

Orexin signaling is implicated in olfactory function. Injection of orexin into the cerebrospinal fluid of the rat brain promoted odor sensitivity and odor sniffing^{33,34}, and orexin modulated the electrical activity of olfactory bulb neurons^{35,36}. However, the mechanism by which orexin signaling in olfactory cortical regions regulates odor-guided appetitive behavior was unknown.

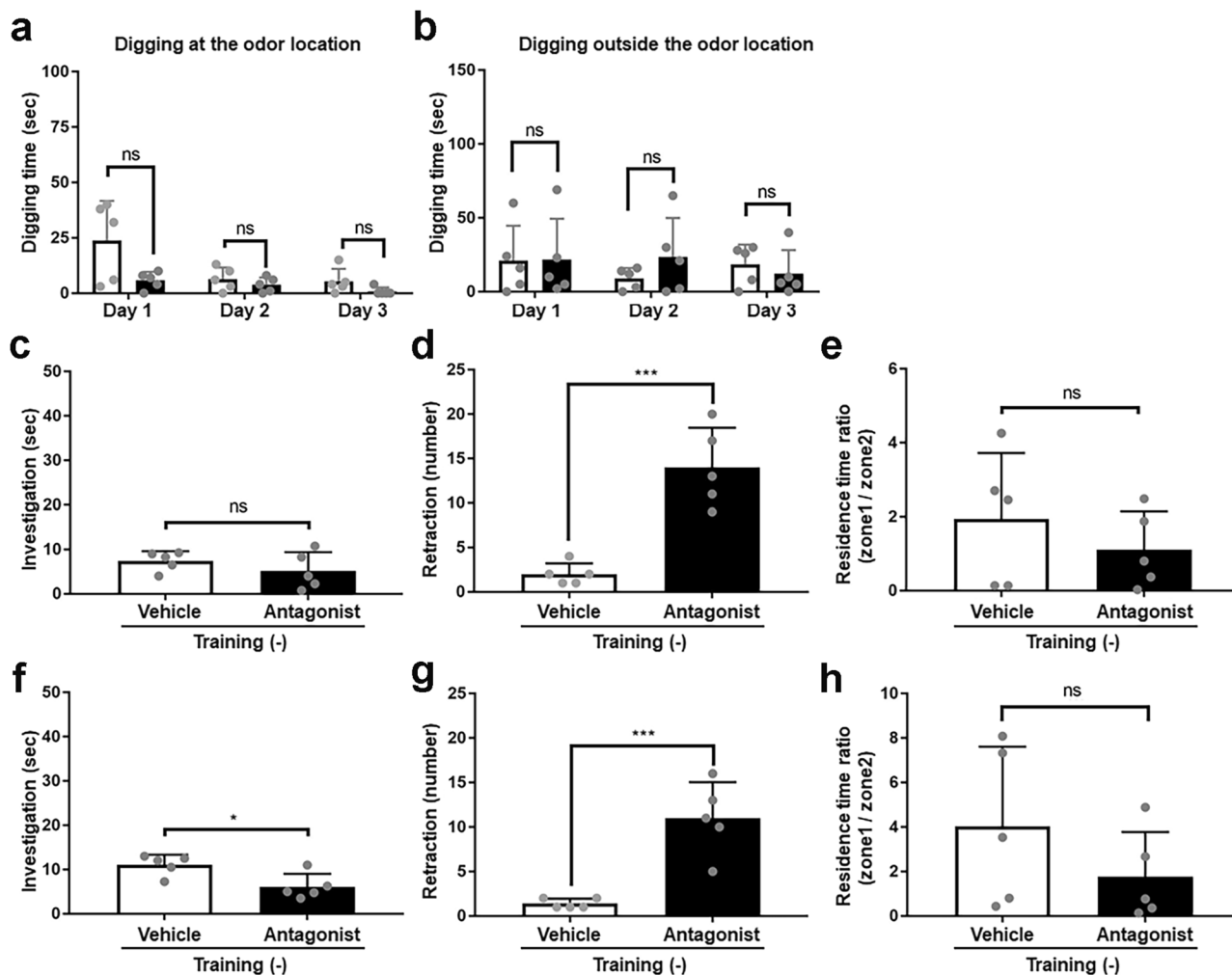


Fig. 5 | Conversion of the unassociated odor valence from neutral to aversion by local injection of an OxR1 antagonist into the amOT. **a, b** Odor-guided behavior of mice during test days 1–3. **a** Digging behavior at the odor location. **b** Digging behavior outside the odor location. Digging time within four 2 min-trials of vehicle-injected mice (white columns) and antagonist-injected mice (black columns). **c–e** Odor-guided behavior of food-restricted mice under the bedding-free condition. **c** Odor-investigating time within 2 min of vehicle-injected mice (white column) and antagonist-injected mice (black column). **d** Occurrence of odor-retraction within

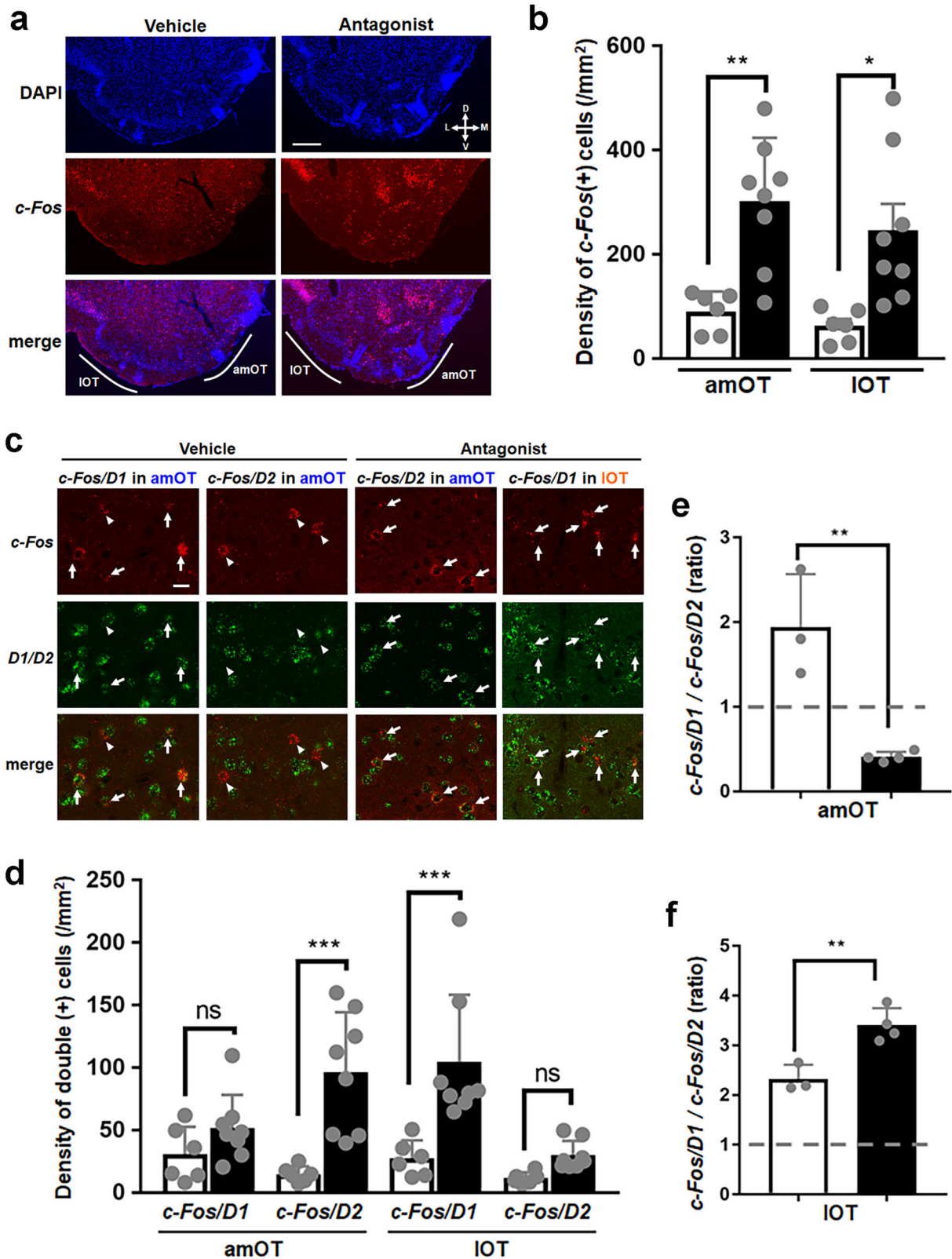
2 min of two groups of mice. **e** Ratio of residence times on the odor side (zone 1) versus the opposite side (zone 2) of two groups of mice. **f–h** Odor-guided behavior of *ad libitum*-fed mice under the bedding-free condition. **f** Odor-investigating time within 2 min of vehicle-injected mice (white column) and antagonist-injected mice (black column). **g** Occurrence of odor-retraction within 2 min of two groups of mice. **h** Ratio of residence times on the odor side (zone 1) versus the opposite side (zone 2) of two groups of mice. Average \pm SD, each dot represents one mouse ($n = 5$ for both groups of mice). ns, not significant; * $p < 0.05$; *** $p < 0.001$ (*t*-test).

In this study, the suppressive effect of injection of an OxR1 antagonist into the amOT on odor-attractive behavior was evident on the first day of the test period; indeed, 30 min after injection (Fig. 1). This immediate effect might underlie our experience in daily food eating, in which preferred food odors become less appetitive when we are satiated. Attenuating this effect within a day also fits with our experience that food odor valence changes many times per day according to hunger/satiety status. Further, the effect of antagonist injection appeared to be potentiated during 3 days of test period, implicating the OT in odor valence and behavior learning^{13,14,24,25,37}. The OT may thus facilitate the adaptive learning of odor valence by integrating odor information and metabolic signals.

Digging behavior of rodents is promoted by various motivations, including food searching, covering the sources of noxious stimuli (defensive burying), and burrowing for shelter^{28,29}. The digging behavior of vehicle-injected mice towards the cue odor was food-searching behavior^{14,30}. The digging behavior of antagonist-injected mice outside cue-odor location could be food-searching behavior directed away from the odor, because this behavior was attenuated under the well-fed condition (Fig. 2h). This behavior, typically opposite to the location of the odor, seemed to involve motivation to escape from the odor, which was supported by its resemblance

to burrowing behavior, in which rodents build shelters to escape from danger, e.g., a predator^{29,31,32}. In this study, antagonist-injected mice dug bedding, beneath which they hid their body and head. While the precise meaning of this aberrant behavior remains unknown, it was likely promoted by the motivation to avoid the cue odor. Indeed, under the bedding-free condition mice slowly approached and rapidly withdrew (whole-body flinch) from the cue odor—a typical odor-aversive behavior^{14,38}. The aversive response to the cue odor additionally indicated that injection of the antagonist did not significantly affect the detectability of the odor. The antagonist-injected mice sensed and responded to the odor differently from the vehicle-injected mice.

Although unexpected, the conversion of odor valence from attraction to aversion and from neutral to aversion by the antagonist injection indicated that the extent of OxR1 signaling in the amOT can positively and negatively modulate odor valence. This notion agrees with the observation that amOT expresses receptors for both appetite-promoting and -suppressing neuromodulators at high levels¹⁵. We believe that many feeding-related neuromodulatory signals act in concert on the amOT to control odor valence in accordance with metabolic status. The lack of an effect of injection of the OxR1 antagonist in the IOT (Fig. 3) is consistent with our report of low



OxR1 expression in the IOT¹⁵. Although orexin and OxR1 in the NAc are implicated in motivational behaviors such as alcohol drinking and drug abuse^{39,40}, injection of the OxR1 antagonist into the NAc did not influence odor-guided attractive behavior (Fig. 4). This might be caused by the functional difference of the OT and NAc in rewarding behavior⁴¹ or the use of different sensory cues (e.g., odor, tone). Although further investigation is

needed, our finding suggests the specific functions of the amOT in regulating odor-guided appetitive behavior in accordance with metabolic status.

Electrophysiological studies of the OT have shown that odor valence is preferentially represented by D1 cell activity in a learning-dependent manner^{24,25}. Histological analysis of *c-Fos*(+) cells showed that odor-guided

Fig. 6 | Effect on cell type- and domain-specific activation in the OT of local injection of an OxR1 antagonist into the amOT. a *c-Fos*(+) cells in the OT of vehicle-injected (left) and antagonist-injected (right) mice. Red, *c-Fos*; blue, DAPI. D, dorsal; V, ventral; M, medial; L, lateral. Scale bar, 500 μ m. **b** *c-Fos*(+) cell density in the amOT and IOT of vehicle-injected (white columns) and antagonist-injected (black columns) mice. **c** *c-Fos/D1* and *c-Fos/D2* double-positive cells in the amOT and IOT of vehicle-injected and antagonist-injected mice. (Leftmost column) *c-Fos/D1* co-detection in the amOT of a vehicle-injected mouse. (Second-left column) *c-Fos/D2* co-detection in the amOT of a vehicle-injected mouse. (Second-right column) *c-Fos/D2* co-detection in the amOT of an antagonist-injected mouse. (Rightmost column) *c-Fos/D1* co-detection in the IOT of an antagonist-injected mouse. Red, *c-Fos* mRNA; green, *D1/D2* mRNA. Double-positive cells (arrows) and *c-Fos*-single-positive cells (arrowheads) are indicated. Scale bar, 10 μ m. **d** Densities

of *c-Fos/D1* and *c-Fos/D2* double-positive cells in the amOT and IOT of vehicle-injected (white columns) and antagonist-injected (black columns) mice. **e** Ratios of *c-Fos/D1* cell density versus *c-Fos/D2* cell density in the amOT of vehicle-injected (white column) and antagonist-injected (black column) mice. A dotted line indicates the ratio at 1. **f** Ratios of *c-Fos/D1* cell density versus *c-Fos/D2* cell density in the IOT of vehicle-injected (white column) and antagonist-injected (black column) mice. A dotted line indicates the ratio at 1. **b, d, e, f** Average \pm SD; ns, not significant; * $p < 0.05$; ** $p < 0.01$; *** $p < 0.001$. **b, d** $n = 6$ from left/right OTs of 3 mice for vehicle-injected mice, $n = 8$ from left/right OTs of 4 mice for antagonist-injected mice (one-way ANOVA with Tukey's multiple comparison test). **e, f** Each dot represents a ratio within each mouse; 3 vehicle-injected mice, 4 antagonist-injected mice (*t*-test).

attractive and aversive behavior learning accompanied preferential activation of D1 cells in the amOT and IOT, respectively¹⁴. Further, optogenetic manipulation showed that activation of D1 cells in the amOT induced attractive behavior whereas activation of D2 cells in the amOT induced aversive behavior²⁷. These observations indicate that D1 cells in the OT promote motivated behaviors and suggest that D2 cells in the OT play complementary roles to D1 cells, as in the NAc⁴². In this study, odor-aversive mice injected with the antagonist in the amOT showed increased activation of D2 cells in the amOT and preferential activation of D1 cells in the IOT (Fig. 6). These observations are consistent with the above-mentioned domain- and cell type-specific regulation of motivated behaviors in the OT. Therefore, metabolic signals in the amOT optimize odor-guided motivated behaviors via the regulation of cell type- and domain-specific OT activation.

The neural mechanism underlying the cell type- and domain-specific regulation by OxR1 signaling is unknown. Our preliminary ISH experiments did not yield reliable results on cell types (D1 or D2 cells) expressing OxR1, mainly because of its low level of expression in the OT compared to other brain regions like hypothalamus. The fact that injection of the antagonist into the amOT influenced activation in the IOT raises the possibility that these OT domains interact. In addition to the topographic projection from the medial/lateral part of the OT to the medial/lateral part of the ventral pallidum⁴³, the medial/lateral OT could show structural and functional interactions. Alternatively, association learning of odor information with altered OxR1 signaling in the amOT might have induced a secondary plastic change in the IOT to potentiate the odor-aversive behavior. The connectivity of orexin neurons to D1 and/or D2 cells in the amOT and IOT is important to understand the physiological control of OT activity by orexin signals. Further studies are needed to evaluate the functions of interactions of the OT domains in the adaptive regulation of odor valence and olfactory behavior.

Consistent odor attraction and aversion both in food restricted and *ad libitum* feeding mice indicates that regulation of odor valence by OxR1 signaling in the amOT may, in principle, be independent of the overall regulation of appetite. During food restriction, antagonist-injected mice ate all the available food and maintained an appropriate body weight (80–90% of that under *ad libitum* feeding), as did vehicle-injected mice, and their body weight recovered to baseline within 1 day of *ad libitum* feeding. Orexin neurons in the lateral hypothalamus are heterogeneous and a subpopulation projects to the olfactory bulb^{44,45}. A subpopulation of orexin neurons might project to the OT domains and regulate odor valence independently of overall feeding motivation. This suggests that modulating orexin signaling in the olfactory system, including the OT, could ameliorate eating disorders linked to like/dislike of food objects⁴⁶.

Reward-related behaviors are typically more closely associated with OxR1 activation whereas sleep/wake regulation is more closely associated with OxR2¹⁷. Regarding orexin signaling in the NAc, excessive alcohol drinking and abuse drug-induced place preference were selectively or more potently suppressed by local injection of an OxR1 antagonist compared to an OxR2 antagonist^{39,40}. Our finding on the function of OxR1 signaling in the amOT in regulating odor valence and odor-guided behavior fits the

general understanding of the function of OxR1. OxR2 is expressed in several OT domains with higher expression in the amOT, but the extent of the domain difference is not as prominent as in OxR1¹⁵. Further investigation of OxR2 signaling in the OT may provide insight into the overall functions of orexin signaling in OT domains.

The OT functions by interacting with other brain regions. The paraventricular thalamus (PVT) receives metabolic signals from the hypothalamus and mediates metabolic state-dependent olfactory behavior⁴⁷. The PVT projects to the limbic area including the OT^{48,49}. The prefrontal cortex participates in the control of feeding behavior via association learning, in which hypothalamic orexigenic signals are involved⁵⁰. OxR1 signaling within the medial prefrontal cortex is necessary for cue-potentiated feeding⁵¹. The OT also receives many projections from the prefrontal cortex^{52,53}. Synaptic information from several brain regions and hormonal information from the hypothalamus and body might converge in OT domains and direct appropriate odor-guided feeding behavior. Further understanding of the function of the OT in the neural network involving the hypothalamus, thalamus, and prefrontal cortex^{50,54} may provide insight into the neural mechanisms of the adaptive control of odor-guided feeding behavior.

Methods

Animals

The experiments were conducted in accordance with the guidelines of the Physiological Society of Japan and were approved by the Animal Care and Use Committee of Kochi Medical School. Male C57BL/6 mice (Japan SLC Inc., Sizuoka, Japan) were housed individually in plastic cages (24 \times 17 \times 12 cm) with wood shavings at 26 $^{\circ}$ C under a 12-h light/dark cycle (lights on at 21:00; off at 9:00). We have complied with all relevant ethical regulations for animal use. Experimental protocols were designed before the study, and animals were randomly assigned to the various experimental groups.

Implantation of drug cannulae

Stereotaxic surgery was performed on 8-week-old mice. The mice were anesthetized with a mixture of three anesthetics (0.3 mg/kg medetomidine, 4 mg/kg midazolam, and 5 mg/kg butorphanol) and placed in a stereotaxic apparatus. The skull was exposed and drilled to make a small hole at the position of cannula implantation. Especially for the implantation in bilateral amOT, bone just at the midline was left intact to avoid damage to midline vessels. Stainless steel 26-gauge guide cannulae (1.8 cm in length) with a 31-gauge obturator were implanted into the bilateral amOT (2.0 mm anterior to the bregma, 0.3 mm lateral to the midline, 4.0 mm deep to the brain surface), IOT (1.9 mm anterior to the bregma, 1.4 mm lateral to the midline, 4.0 mm deep to the brain surface), or NAc shell (2.0 mm anterior to the bregma, 0.7 mm lateral to the midline, 3.2 mm deep to the brain surface). Tip of the obturator protruded by 1 mm from the guide cannula (the depth of the cannula coordinate described above indicates that of the obturator tip). The cannulae were fixed to the skull using dental acrylic, and covered by a plastic cup made from a 15 ml plastic tube (Supplementary Fig. 1).

OxR1 antagonist preparation and injection

SB334867 (Tocris Bioscience, Bristol, UK), a selective OxR1 antagonist, was dissolved at 5.3 $\mu\text{g}/\mu\text{L}$ in artificial cerebrospinal fluid (aCSF; 125 mM NaCl, 25 mM NaHCO_3 , 3 mM KCl, 1 mM NaH_2PO_4 , 1 mM MgCl_2 , 15 mM glucose, and 2 mM CaCl_2 at pH 7.4) containing 33% dimethyl sulfoxide (DMSO) and 30% 2-hydroxy- β -cyclodextrin. Mice were gently held by an experimenter, and the obturator of the drug cannula was removed to insert 31-gauge inner cannula connected to a syringe pump (SP101i, World Precision Instruments Inc., Sarasota, FL, USA) with polyethylene tubes (SP10 and SP19, Natsume Seisakusho Co., Ltd., Tokyo, Japan) (Supplementary Fig. 1). The tip of the inner cannula was designed to protrude by 1 mm from the guide cannula. Drug solution was injected at 0.08 $\mu\text{L}/\text{min}$ for 5 min (0.4 μL total) from each cannula. After being held for additional 5 min (holding \sim 15 min in total), the mice were returned to their home cages. For vehicle injection, aCSF with 33% DMSO and 30% 2-hydroxy- β -cyclodextrin was used. The injection volume was determined by preliminary fluorescent molecule injection and our previous viral injection study²⁷, with which injected solution and virus-mediated molecule expression spread within the am/LOT.

Odor and sugar association training

After 2 weeks of recovery from cannula implantation, mice were food-restricted to achieve 80–90% of their body weight while feeding *ad libitum*. Food restriction started 2 days prior to odor-sugar association training. A limited amount of food pellets (2.7–3.3 g per day) was provided to maintain 80–90% body weight during the training period; water was available *ad libitum*. Association training was conducted in a plastic conditioning cage (24 \times 17 \times 12 cm) with 2-cm-deep white paper bedding (Japan SLC Inc.). On day 1 of training, mice learned to eat sugar; they were presented with sugar (granulated sucrose; 20–40 mg) together with powdered diet (20–40 mg) on a Petri dish, and subsequently with sugar alone (50 mg). Next, the mice underwent association training of the sugar reward and a cue odor. Sugar (50 mg) was placed on a Petri dish with holes exposing filter paper (2 \times 2 cm) soaked with 10 μL of eugenol (Tokyo Chemical Industry, Tokyo, Japan) in the lower compartment. The dish was placed on the paper bedding for mice to eat sugar while sensing eugenol odor, a procedure repeated three times. On training days 2–4, the dish was hidden under the bedding (2 cm depth) so that the mouse could locate it by smell, and the position of the hidden dish within the conditioning cage was chosen randomly. Because mice could find and eat the sugar within 2 min, the duration of one trial was fixed at 2 min. Four training trials per day were conducted. For mice without odor-sugar association training, the same food restriction was applied, and a holed Petri dish containing filter paper soaked with 10 μL of eugenol without sugar was presented for one 2 min trial. Four trials per day were conducted on training days 1–4.

OxR1 injection and behavior analysis

After 4 days of odor-sugar association training, the effect of injection of an OxR1 antagonist on odor-guided behavior was examined. On the first day of the test period (test day 1), mice were habituated to a larger test cage (30 \times 20 \times 13 cm) with paper bedding (2 cm depth) for 30 min. Next, the mice were injected with OxR1 antagonist or vehicle into the bilateral amOT, LOT, or NAc shell via the drug cannulae. After 30 min of rest in their home cages, the mice were transferred to the test cages in which dishes scented with 10 μL of eugenol, but without sugar, were buried under the bedding. The digging behavior of the mice was recorded on video for 2 min and analyzed off-line. Digging behavior over the buried dish was evaluated as *digging at the odor location* and digging behavior elsewhere as *digging outside the odor location*, and the total digging time in the 2 min trial was calculated. The trial was repeated four times at 1 min intervals. The total digging time of four trials was determined and evaluated. The procedure was repeated on two consecutive days (test days 2–3).

On test day 4, the mice were habituated to a test cage (30 \times 20 \times 13 cm) without paper bedding. Then, the mice were injected with OxR1 antagonist or vehicle via the drug cannulae. After 30 min of rest in their home cages, the

mice were transferred to test cages in which a dish scented with 10 μL of eugenol without sugar was placed on the cage. The behavior of the mice was recorded on video for 2 min and analyzed off-line. Behavior was assigned as *investigating the odor* when a mouse brought its nose close to the dish ($<$ 1 cm) and appeared to pay attention to the odorized dish. Behavior was assigned as *retraction from the odor* when a mouse initially showed approaching behavior toward the odorized dish and then rapidly retracted its nose and body in the opposite direction (whole-body flinch)^{14,38}. The cage space was divided at the midline into two zones—the odor side (zone 1) and the opposite side (zone 2). Residence time within each zone was calculated using SMART ver. 3.0 software (Panlab, Barcelona, Spain).

After the day-4 test, mice were supplied with sufficient food. After \sim 24 h of *ad libitum* feeding (test day 5), the mice underwent the same procedure as test day 4—habituation to a test cage, injection of OxR1 antagonist or vehicle, and analysis of behavior in response to odor presentation. In one experiment (Fig. 2g–k), mice were supplied with sufficient food after 4 days of odor-associating training and underwent test of days 1–4. No specific randomization was adopted in behavioral analyses. This study did not set humane endpoints.

Histological analysis

On the day after completion of behavioral analyses, mice were injected with OxR1 antagonist or vehicle via the drug cannulae. After 30 min, the behavior of the mice in response to odor presentation was evaluated in test cages as on test days 4–5. At 1 h after the first odor presentation, mice were deeply anesthetized via intraperitoneal injection of sodium pentobarbital (150 mg/kg), and transcardially perfused with phosphate-buffered saline (PBS) followed by 4% paraformaldehyde (PFA) in 0.1 M phosphate buffer (PB). The brains were removed from the skull, immersed in 4% PFA overnight, and transferred to 30% sucrose in 0.1 M PB. The brains were next embedded in optimal cutting temperature compound (Sakura Finetek, Tokyo, Japan), frozen at -80°C , and cut into coronal sections at a thickness of 20 μm using a cryotome. The sections were mounted on glass slides. The locations of the drug cannulae were confirmed under a fluorescence microscope after staining the sections with 4',6-diamidino-2-phenylindole (DAPI; 2 $\mu\text{g}/\text{mL}$).

In situ hybridization (ISH)

Plasmid templates for in vitro transcription for *D1* and *D2* mRNAs were kindly provided by Dr. Kazuto Kobayashi⁵⁵, and that for *c-Fos* mRNA was kindly provided by Dr. Hirohide Takebayashi⁵⁶. We prepared fluorescein (FLU)-labeled RNA probes for *D1* and *D2* mRNAs and digoxigenin (DIG)-labeled RNA probes for *c-Fos* mRNAs using an in vitro transcription kit (Roche, Basel, Switzerland) according to the manufacturer's protocol.

ISH using two fluorescent probes was conducted according to a published protocol⁵⁷ with minor modifications. Coronal sections were fixed in 4% PFA for 20 min, digested with proteinase K (10 $\mu\text{g}/\text{mL}$) for 30 min, and post-fixed in 4% PFA for 15 min. After pre-hybridization, the sections were incubated overnight at 65°C with FLU-labeled and DIG-labeled RNA probes. After stringent washing, blocking was performed in 1% blocking buffer (FP1020, Akoya Biosciences, Marlborough, MA, USA). For detection of FLU-labeled probes, the sections were incubated with an anti-FLU antibody conjugated to horseradish peroxidase (1:500; Roche) for 1 h at room temperature. After 5 min wash in Tris-NaCl-Tween 20 (TNT) buffer (0.1 M Tris-HCl, pH 7.5; 0.15 M NaCl; 0.1% Tween 20), the sections were treated with diluted (1:100) Tyramide Signal Amplification (TSA)-Plus FITC reagents for 10 min according to the manufacturer's instructions (Akoya Biosciences), and the FLU signals were converted to FITC signals. The sections were next washed two times in TNT for 5 min each and incubated in 0.02 N HCl in saline for 30 min at room temperature to inactivate peroxidase activity, which is associated with detection of previous RNA probes. To detect DIG-labeled probes, the sections were incubated with an anti-DIG antibody conjugated with horseradish peroxidase (1:500; Roche) overnight at 4°C . After 5 min wash in TNT, the sections were treated with diluted (1:100) TSA-Plus Cy3 reagents for 10 min according to the manufacturer's instructions (Akoya Biosciences), and the DIG signals were

converted to Cy3 signals. The sections were washed two times in TNT for 5 min each, counterstained with DAPI diluted in PBS (2 µg/mL) for 5 min, and mounted (Prolong Gold; Thermo Fisher Scientific, Waltham, MA, USA).

Image acquisition and quantification

Image acquisition and quantification of *c-Fos*(+), *c-Fos/DI*(+), and *c-Fos/D2*(+) cells were conducted using a fluorescence microscope (DM600B; Leica, Wetzlar, Germany) and a confocal microscope (SP5; Leica). To enumerate cells in the OT domain, serial coronal sections (20 µm thickness) of the OT were selected at a rate of 1 in 10 and those containing amOT or IOT were analyzed. amOT and IOT were identified as described previously, using Islands of Calleja and cap compartments as landmarks^{14,37}. On average, we selected three sections for amOT and three sections for IOT for each mouse brain, and the densities of *c-Fos*(+), *c-Fos/DI*(+), and *c-Fos/D2*(+) cells in the amOT (layer II) and IOT (layer II) were analyzed.

Statistics and reproducibility

Statistical analysis was performed using Prism software (ver. 7.04; GraphPad Software, Inc., La Jolla, CA, USA) and IBM SPSS Statistics software (ver. 23.0; IBM Corp., Armonk, NY, USA). Graphs were plotted using Prism software. Two-way repeated measures of analysis of variance (ANOVA) (one repeated measures factor for “day” and one non-repeated measures factor for “injection”) was used for the evaluation of digging behavior across days, and the two-tailed Student’s *t*-test was used for comparisons between vehicle and antagonist injections in each day. One-way ANOVA followed by Tukey’s multiple comparisons test was used for comparisons among more than three groups. The two-tailed Student’s *t*-test was used for comparisons between two groups. Statistical significance was set at $p < 0.05$. Numbers of replicates were determined by referencing similar foregoing manuscripts and indicated per experiment in the figure captions and in the respective parts of the Results section.

Data availability

The source data for the graphs in the paper can be found in the Supplementary Data file. All data supporting the findings described in this manuscript are available from the corresponding author upon reasonable request.

Received: 1 May 2024; Accepted: 23 December 2024;

Published online: 26 December 2024

References

- Doty, R. L. Odor-guided behavior in mammals. *Experientia* **42**, 257–271 (1986).
- Rolls, E. T. Reward systems in the brain and nutrition. *Annu. Rev. Nutr.* **36**, 435–470 (2016).
- Ferrario, C. R. et al. Homeostasis meets motivation in the battle to control food intake. *J. Neurosci.* **36**, 11469–11481 (2016).
- Waterson, M. J. & Horvath, T. L. Neuronal regulation of energy homeostasis: beyond the hypothalamus and feeding. *Cell Metab.* **22**, 962–970 (2015).
- Julliard, A. K., Al Koborssy, D., Fadool, D. A. & Palouzier-Paulignan, B. Nutrient sensing: another chemosensitivity of the olfactory system. *Front. Physiol.* **8**, 468 (2017).
- Palouzier-Paulignan, B. et al. Olfaction under metabolic influences. *Chem. Senses* **37**, 769–797 (2012).
- Neville, K.R. & Haberly, L.B. Olfactory Cortex. in *The synaptic organization of the brain, 5th edition* (ed. Shepherd, G.M.) 415–454 (Oxford University Press, 2004).
- Ikemoto, S. Dopamine reward circuitry: two projection systems from the ventral midbrain to the nucleus accumbens-olfactory tubercle complex. *Brain Res. Rev.* **56**, 27–78 (2007).
- Wesson, D. W. The tubular striatum. *J. Neurosci.* **40**, 7379–7386 (2020).
- Wesson, D. W. & Wilson, D. A. Sniffing out the contributions of the olfactory tubercle to the sense of smell: hedonics, sensory integration, and more? *Neurosci. Biobehav. Rev.* **35**, 655–668 (2011).
- DiBenedictis, B. T., Olugbemi, A. O., Baum, M. J. & Cherry, J. A. DREADD-Induced silencing of the medial olfactory tubercle disrupts the preference of female mice for opposite-sex chemosignals(1,2,3). *eNeuro* **2**, 1–16 (2015).
- Fitzgerald, B. J., Richardson, K. & Wesson, D. W. Olfactory tubercle stimulation alters odor preference behavior and recruits forebrain reward and motivational centers. *Front. Behav. Neurosci.* **8**, 81 (2014).
- Gadziola, M. A., Tylicki, K. A., Christian, D. L. & Wesson, D. W. The olfactory tubercle encodes odor valence in behaving mice. *J. Neurosci.* **35**, 4515–4527 (2015).
- Murata, K., Kanno, M., Ieki, N., Mori, K. & Yamaguchi, M. Mapping of learned odor-induced motivated behaviors in the mouse olfactory tubercle. *J. Neurosci.* **35**, 10581–10599 (2015).
- Nogi, Y. et al. Expression of feeding-related neuromodulatory signalling molecules in the mouse central olfactory system. *Sci. Rep.* **10**, 890 (2020).
- Boutrel, B., Steiner, N. & Halfon, O. The hypocretins and the reward function: what have we learned so far?. *Front. Behav. Neurosci.* **7**, 59 (2013).
- Mahler, S. V., Moorman, D. E., Smith, R. J., James, M. H. & Aston-Jones, G. Motivational activation: a unifying hypothesis of orexin/hypocretin function. *Nat. Neurosci.* **17**, 1298–1303 (2014).
- Milbank, E. & López, M. Orexins/Hypocretins: key regulators of energy homeostasis. *Front. Endocrinol.* **10**, 830 (2019).
- Peyron, C. et al. Neurons containing hypocretin (orexin) project to multiple neuronal systems. *J. Neurosci.* **18**, 9996–10015 (1998).
- Sakurai, T. et al. Orexins and orexin receptors: a family of hypothalamic neuropeptides and G protein-coupled receptors that regulate feeding behavior. *Cell* **92**, 573–585 (1998).
- Caillol, M., Aioun, J., Baly, C., Persuy, M. A. & Salesse, R. Localization of orexins and their receptors in the rat olfactory system: possible modulation of olfactory perception by a neuropeptide synthesized centrally or locally. *Brain Res.* **960**, 48–61 (2003).
- Cluderay, J. E., Harrison, D. C. & Hervieu, G. J. Protein distribution of the orexin-2 receptor in the rat central nervous system. *Regul. Pept.* **104**, 131–144 (2002).
- Hervieu, G. J., Cluderay, J. E., Harrison, D. C., Roberts, J. C. & Leslie, R. A. Gene expression and protein distribution of the orexin-1 receptor in the rat brain and spinal cord. *Neuroscience* **103**, 777–797 (2001).
- Gadziola, M. A. et al. A neural system that represents the association of odors with rewarded outcomes and promotes behavioral engagement. *Cell Rep.* **32**, 107919 (2020).
- Martiros, N., Kapoor, V., Kim, S.E. & Murthy, V.N. Distinct representation of cue-outcome association by D1 and D2 neurons in the ventral striatum’s olfactory tubercle. *Elife* **11**, e75463 (2022).
- White, K. A. et al. Glutamatergic neurons in the piriform cortex influence the activity of D1- and D2-Type Receptor-expressing olfactory tubercle neurons. *J. Neurosci.* **39**, 9546–9559 (2019).
- Murata, K. et al. Opposing roles of dopamine Receptor D1- and D2-Expressing neurons in the anteromedial olfactory tubercle in acquisition of place preference in mice. *Front. Behav. Neurosci.* **13**, 50 (2019).
- De Boer, S. F. & Koolhaas, J. M. Defensive burying in rodents: ethology, neurobiology and psychopharmacology. *Eur. J. Pharmacol.* **463**, 145–161 (2003).
- Pond, H. L. et al. Digging behavior discrimination test to probe burrowing and exploratory digging in male and female mice. *J. Neurosci. Res.* **99**, 2046–2058 (2021).

30. Machado, C. F., Reis-Silva, T. M., Lyra, C. S., Felicio, L. F. & Malnic, B. Buried food-seeking test for the assessment of olfactory detection in mice. *Bio Protoc.* **8**, e2897 (2018).
31. Fucich, E.A. & Morilak, D.A. Shock-probe defensive burying test to measure active versus passive coping style in response to an aversive stimulus in rats. *Bio Protoc.* **8**, e2998–e2998 (2018).
32. Harper, S. J. & Batzli, G. O. effects of predators on structure of the burrows of voles. *J. Mammal.* **77**, 1114–1121 (1996).
33. Julliard, A. K. et al. Changes in rat olfactory detection performance induced by orexin and leptin mimicking fasting and satiation. *Behav. Brain Res.* **183**, 123–129 (2007).
34. Prud'homme, M. J. et al. Nutritional status modulates behavioural and olfactory bulb Fos responses to isoamyl acetate or food odour in rats: roles of orexins and leptin. *Neuroscience* **162**, 1287–1298 (2009).
35. Apelbaum, A. F., Perrut, A. & Chaput, M. Orexin A effects on the olfactory bulb spontaneous activity and odor responsiveness in freely breathing rats. *Regul. Pept.* **129**, 49–61 (2005).
36. Hardy, A. B. et al. Orexin A modulates mitral cell activity in the rat olfactory bulb: patch-clamp study on slices and immunocytochemical localization of orexin receptors. *Endocrinology* **146**, 4042–4053 (2005).
37. Sha, M. F. R., Koga, Y., Murata, Y., Taniguchi, M. & Yamaguchi, M. Learning-dependent structural plasticity of intracortical and sensory connections to functional domains of the olfactory tubercle. *Front. Neurosci.* **17**, 1247375 (2023).
38. Crawley, J. N. Behavioral phenotyping strategies for mutant mice. *Neuron* **57**, 809–818 (2008).
39. Amirteymori, H. et al. Hypocretin/orexin system in the nucleus accumbens as a promising player in the extinction and reinstatement of methamphetamine-induced CPP. *Prog. Neuropsychopharmacol. Biol. Psychiatry* **120**, 110616 (2023).
40. Lei, K. et al. Nucleus accumbens shell and mPFC but not Insula Orexin-1 receptors promote excessive alcohol drinking. *Front. Neurosci.* **10**, 400 (2016).
41. Wright, K. N. & Wesson, D. W. The tubular striatum and nucleus accumbens distinctly represent reward-taking and reward-seeking. *J. Neurophysiol.* **125**, 166–183 (2021).
42. Hikida, T., Morita, M. & Macpherson, T. Neural mechanisms of the nucleus accumbens circuit in reward and aversive learning. *Neurosci. Res.* **108**, 1–5 (2016).
43. Heimer, L., Zaborszky, L., Zahm, D. S. & Alheid, G. F. The ventral striatopallidothalamic projection: I. The striatopallidal link originating in the striatal parts of the olfactory tubercle. *J. Comp. Neurol.* **255**, 571–591 (1987).
44. Qi, M., Fadool, D. A. & Storace, D. A. An anatomically distinct subpopulation of orexin neurons project from the lateral hypothalamus to the olfactory bulb. *J. Comp. Neurol.* **531**, 1510–1524 (2023).
45. Sagi, D., de Lecea, L. & Appelbaum, L. Heterogeneity of Hypocretin/Orexin Neurons. *Front. Neurol. Neurosci.* **45**, 61–74 (2021).
46. Islam, M. A. et al. Olfaction in eating disorders and abnormal eating behavior: a systematic review. *Front. Psychol.* **6**, 1431 (2015).
47. Horio, N. & Liberles, S. D. Hunger enhances food-odour attraction through a neuropeptide Y spotlight. *Nature* **592**, 262–266 (2021).
48. Moga, M. M., Weis, R. P. & Moore, R. Y. Efferent projections of the paraventricular thalamic nucleus in the rat. *J. Comp. Neurol.* **359**, 221–238 (1995).
49. Vertes, R. P. & Hoover, W. B. Projections of the paraventricular and paratenial nuclei of the dorsal midline thalamus in the rat. *J. Comp. Neurol.* **508**, 212–237 (2008).
50. Petrovich, G. D. Forebrain networks and the control of feeding by environmental learned cues. *Physiol. Behav.* **121**, 10–18 (2013).
51. Cole, S., Keefer, S. E., Anderson, L. C. & Petrovich, G. D. Medial prefrontal cortex neural plasticity, Orexin Receptor 1 signaling, and connectivity with the lateral hypothalamus are necessary in cue-potentiated feeding. *J. Neurosci.* **40**, 1744–1755 (2020).
52. Berendse, H. W., Galis-de Graaf, Y. & Groenewegen, H. J. Topographical organization and relationship with ventral striatal compartments of prefrontal corticostriatal projections in the rat. *J. Comp. Neurol.* **316**, 314–347 (1992).
53. Cansler, H. L. et al. Organization and engagement of a prefrontal-olfactory network during olfactory selective attention. *Cereb. Cortex* **33**, 1504–1526 (2023).
54. Iglesias, A. G. & Flagel, S. B. The paraventricular thalamus as a critical node of motivated behavior via the hypothalamic-thalamic-striatal circuit. *Front. Integr. Neurosci.* **15**, 706713 (2021).
55. Sano, H. et al. Conditional ablation of striatal neuronal types containing dopamine D2 receptor disturbs coordination of basal ganglia function. *J. Neurosci.* **23**, 9078–9088 (2003).
56. Bepari, A. K., Watanabe, K., Yamaguchi, M., Tamamaki, N. & Takebayashi, H. Visualization of odor-induced neuronal activity by immediate early gene expression. *BMC Neurosci.* **13**, 140 (2012).
57. Maegawa, A., Murata, K., Kuroda, K., Fujieda, S. & Fukazawa, Y. Cellular profiles of Prodynorphin and Preproenkephalin mRNA-expressing neurons in the anterior olfactory tubercle of mice. *Front. Neural Circuits* **16**, 908964 (2022).

Acknowledgements

M.Y. was supported for the research of this work from Grants-in-Aid for Scientific Research from Japan Society for the Promotion of Science (Nos. 19H03341 and 22H02734) and by Research Grant from Urakami Foundation for Food and Food Culture Promotion. We thank Dr. Koshi Murata in the Division of Brain Structure and Function, Faculty of Medical Sciences, University of Fukui for support and advice with ISH analysis. We thank all members of the Department of Physiology, Kochi Medical School for their useful discussions and suggestions.

Author contributions

M.M.A. and M.Y. contributed to the initial conception and design of the study. Y.M. and M.T. helped improve the conception and study design. M.M.A., M.T.A., and M.Y. organized and conducted the experiments. M.M.A. and M.T.A. were aware of the group allocation at the different stages of the experiment and M.Y. shared the information. M.M.A. and M.Y. drafted the initial manuscript. All the authors contributed to the improvement of the manuscript and have read and approved the final version.

Competing interests

The authors declare no competing interests.

Additional information

Supplementary information The online version contains supplementary material available at <https://doi.org/10.1038/s42003-024-07438-1>.

Correspondence and requests for materials should be addressed to Masahiro Yamaguchi.

Peer review information *Communications Biology* thanks Markus Rothermel and the other, anonymous, reviewer(s) for their contribution to the peer review of this work. Primary Handling Editor: Christina Karlsson Rosenthal.

Reprints and permissions information is available at <http://www.nature.com/reprints>

Publisher's note Springer Nature remains neutral with regard to jurisdictional claims in published maps and institutional affiliations.

Open Access This article is licensed under a Creative Commons Attribution-NonCommercial-NoDerivatives 4.0 International License, which permits any non-commercial use, sharing, distribution and reproduction in any medium or format, as long as you give appropriate credit to the original author(s) and the source, provide a link to the Creative Commons licence, and indicate if you modified the licensed material. You do not have permission under this licence to share adapted material derived from this article or parts of it. The images or other third party material in this article are included in the article's Creative Commons licence, unless indicated otherwise in a credit line to the material. If material is not included in the article's Creative Commons licence and your intended use is not permitted by statutory regulation or exceeds the permitted use, you will need to obtain permission directly from the copyright holder. To view a copy of this licence, visit <http://creativecommons.org/licenses/by-nc-nd/4.0/>.

© The Author(s) 2024